Performance Optimization of Two-Way AF Relaying in Asymmetric Fading Channels

Qi Yanyan[1], Wang Xiaoxiang[1]
[1] Key Laboratory of Universal Wireless Communications, Ministry of Education, Beijing University of Posts and Telecommunications, Beijing, 100876 - China
[e-mail: thomas_qiyan@bupt.edu.cn, wanginfo@bupt.edu.cn]
*Corresponding author: Qi Yanyan

Received August 15, 2014; revised August 4, 2014; accepted November 20, 2014; published December 31, 2014

Abstract

It is widely observed that in practical wireless cooperative communication systems, different links may experience different fading characteristics. In this paper, we investigate into the outage probability and channel capacity of two-way amplify-and-forward (TWAF) relaying systems operating over a mixed asymmetric Rician and Rayleigh fading scenario, with different amplification policies (AP) adopted at the relay, respectively. As TWAF relay network carries concurrent traffics towards two opposite directions, both end-to-end and overall performance metrics were considered. In detail, both uniform exact expressions and simplified asymptotic expressions for the end-to-end outage probability (OP) were presented, based on which the system overall OP was studied under the condition of the two source nodes having non-identical traffic requirements. Furthermore, exact expressions for tight lower bounds as well as high SNR approximations of channel capacity of the considered scenario were presented. For both OP and channel capacity, with different APs, effective power allocation (PA) schemes under different constraints were given to optimize the system performance. Extensive simulations were carried out to verify the analytical results and to demonstrate the impact of channel asymmetry on the system performance.

Keywords: Two-way relay, variable gain, fixed gain, outage probability, channel capacity, power allocation

This work was supported by the National High Technology Research and Development Program of China (863 Program) under Grant No.2014AA01A701.

http://dx.doi.org/10.3837/tiis.2014.12.011

1. Introduction

Recently, cooperative relay networks have drawn much attention from research community as it provides simple solutions to extend radio coverage and to improve link quality. Of particular interest is the two-way (TW) relay network, compared with conventional one-way (OW) relay network, it brings considerable spectral efficiency improvement as completing one round of bidirectional information exchange in two time slots [1] between two half-duplex terminals. Different transmission protocols employing different signal processing technique can be utilized in cooperative relay networks such as amplify-and-forward (AF), decode-and-forward (DF), compress-and-forward (CF) and so on, among which the AF protocol is a popular concern because it is low-cost and easy to implement while providing satisfactory performance. The relay node in an AF cooperative network may adopt different amplification policies (AP), such as variable gain (VG) policy which requires instantaneous channel state information (CSI) of two incoming links, fixed gain (FG) policy where only statistical channel distribution information (CDI) is needed, and mixed policies where full CSI of one link and CDI of the other link is needed at the relay [2].

During the last few years, much effort has been devoted to evaluate the performance of dual hop relay networks. The authors in [3] investigated into the symbol error probability (SER) for higher order modulation schemes in TW relay network under Rayleigh fading channels when physical layer network coding (PLNC) technique is adopted at the relay. For two-way amplify-and-forward (TWAF) relay network with VG policy under Rayleigh fading channels, when two source terminals have non-identical traffic requirements, the overall system outage probability (OP) was analyzed and then optimized subject to different constraints in [4][5]. By applying a geometric method, the OP of a TWAF VG relay network under Rician fading channels was presented in [6]. As for Nakagami-*m* fading channels, end-to-end performance including OP, channel capacity and SER was analyzed in [7][8] for relay networks with VG and FG polices, respectively. Due to mathematical complexity, the topic of overall system OP in TWAF FG networks was relatively less addressed upon. Recently, Ni etc. [9] presented exact expressions and high signal-to-noise ratio (SNR) approximations of overall OP in TWAF FG relay networks with asymmetric traffic requirements under Rayleigh fading channels. As another important performance measure, channel capacity has been extensively studied as well. Thorough analysis and optimization of achievable rate for different kinds of relay networks were presented in [10] for AF protocol and in [11] for DF protocol, respectively. Generic expressions of upper and lower bounds for channel capacity of dual hop AF relay networks under different fading channels were given in [12][13].

In practical wireless engineering, it is widely observed that different links in wireless cooperative communication systems may experience different fading characteristics, rendering the system to be asymmetric. Performance analysis of such networks has always been a hot topic in the literature. The end-to-end OP and SER of dual hop AF relay networks operating over mixed Rician and Nakagami-*m* fading channels was studied in [14]. In OW relay network operating over mixed shadowed Rician and Nakagami-*m* fading channels, the authors in [15] derived the moment generating function (MGF) of end-to-end SNR. Recently, a mixed generalized $\kappa-\mu$ and $\eta-\mu$ fading scenario is investigated in [16], the end-to-end OP and SER of dual hop AF relay networks with both FG and VG policies were considered.

The special case of mixed Rician and Rayleigh fading scenario is of practical interest in modeling mixed line of sight (LOS) and none-LOS (NLOS) fading channels, which occurs in various wireless applications and is recommended by popular communication standards. The end-to-end OP and SER of dual hop AF relay networks under this special mixed fading scenario is investigated in [17] for VG policy and in [18] for FG policy. The authors in [19] presented asymptotic OP and SER study of an opportunistic TWAF VG relay network where one out of N candidate relays is chosen for transmission. To the best of the authors' knowledge, the overall OP of TWAF relay networks in such a mixed fading scenario where two source nodes have different traffic requirements, along with the topic of channel capacity, under either VG or FG policy, is not seen published in the literature.

Based on the observations above, in this paper, we focus on the analysis and optimization of both the end-to-end and overall OP and channel capacity in a TWAF relay network, operating over mixed Rician and Rayleigh fading channels, with different APs adopted at the relay, respectively. In particular, the main contributions of this paper are summarized as follows:

1. A uniform expression for the cumulative distribution function (CDF) of end-to-end SNR that applies to different APs was presented and simplified asymptotic expressions of end-to-end OP for VG and FG policies were given. Besides, the topic of optimizing the end-to-end OP performance was briefly described.

2. For TWAF relay network where two source nodes have non-identical traffic requirement, with FG policy, a general expression of the overall OP were analyzed and based on which effective power allocation (PA) schemes were obtained via brute-force numerical exhaustive search type algorithms under different constraints, respectively. With VG policy, we were able to obtain the high SNR asymptotic expressions of the overall OP of the considered scenario and then theoretical global optimizers were presented in closed-from under different constraints. Simulation results showed that the proposed PA schemes achieve considerable performance improvements compared to equal power allocation (EPA) scheme. To sum up, a discussion is provided about the similarities and differences between the logic of PA schemes for VG and FG policies.

3. Exact expressions of generic tight lower bounds and high SNR approximations of channel capacity of the considered scenario were presented, with FG and VG policies adopted at the relay, respectively. Global optimizers that maximize the system sum capacity under different constraints are obtained via numerical methods.

4. We compare the performance of TWAF relay network operating in the considered asymmetric scenario with than in a conventional homogenous Rayleigh/Rayleigh fading scenario and a discussion of the impact of the channel asymmetry on system performance was provided.

The rest of the paper is organized as follows, In Section 2 we briefly outline the system and channel model. In Section 3, we give elaborate analysis of end-to-end OP under different APs. The overall OP and PA issue is detailed in Section 4, Section 5 deals with the topic of channel capacity. Finally, we conclude this paper in section 6.

Throughout this paper, $E\{\cdot\}$ and $P\{\cdot\}$ denote the expectation and probability, respectively. Bold italic symbols indicate vectors. $[x]^+ = max\,(0, x)$. $f_\alpha(x)$, $F_\alpha(x)$, $\tilde{F}_\alpha(x) = 1 - F_\alpha(x)$ represents the probability density function (PDF), CDF and complementary CDF (C-CDF) with respect to (w.r.t.) the random variable (RV) α. $\Gamma(a, x)$ and $\Upsilon(a, x)$ stand for the upper and lower incomplete gamma functions ([20], eq. (8.350.1-2)), respectively. $\mathcal{E} \approx 0.577$ is the Euler's constant. $I_v(z)$ and $K_v(z)$ denote the

v-th order modified Bessel functions of the first kind ([20], eq. (8.445)) and second kind ([20], eq. (8.446)), respectively. ${}_pF_q(a_1 \dots a_p; b \dots b_q; z)$ is the generalized hypergeometric function ([20], eq. (9.14.1)). $E_n(x)$ is the generalized exponential integral function ([21], eq. (5.1.4)). $Q_1(\alpha, \beta) = \int_\beta^\infty x exp(-(x^2+\alpha^2)/2)\, I_0(\alpha x) dx$ is the first-order Marcum-Q function ([22], eq. (4.34)).

2. System and Channel Models

The system under consideration is shown in **Fig. 1**. Two terminal nodes, N_1 and N_2, communicate to each other with the aid of a single relay node, R. One round information exchange occupies two time slots. In the first time slot, both N_1 and N_2 transmit their individual data signals simultaneously to the relay. In the second time slot, the relay simply broadcasts an amplified version of the received signal to the two source terminals. The system operates in half-duplex mode and no direct link between N_1 and N_2 is available due to long distance and severe shadowing. Assume independent additive white Gaussian noise (AWGN) with zero-mean and variance N_0 is present at all nodes and all channels are both reciprocal and quasi-static.

To simplify notations, let $\boldsymbol{h} = [h_1\ h_2]$ be the channel coefficient, $\alpha_i = |h_i|^2$, let $\Omega_i = E\{|h_i|^2\}$, $i \in \{1,2\}$ denote the instantaneous and statistical channel power, respectively. E_s indicates the total power constraint during two time slots and $\rho = E_s/N_0$ represents the system SNR. $\boldsymbol{q} = [q_1\ q_2\ q_3]$, $q_1 + q_2 + q_3 = 1$, $q_i > 0$, $i \in \{1,2,3\}$ stands for the PA vector with elements corresponding to N_1, N_2, and R, respectively. Particularly, the logical $N_1 \to R \to N_2$ transmission is termed the forward link and $N_1 \leftarrow R \leftarrow N_2$ transmission the reverse link, respectively.

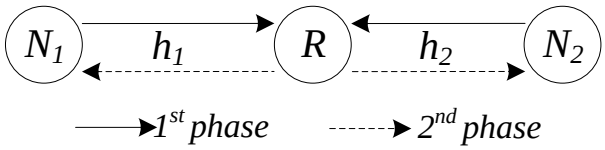

Fig. 1. Two-way relay network model under consideration

In order to incorporate the effect of relay geometry into our analysis, we adopt a simple linear model that R is located somewhere on the line between N_1 and N_2. The distance between N_1 and N_2 is normalized to unity, while the distances between N_1 and R, N_1 and R are denoted as d and $1-d$, respectively. Let υ be the path loss exponent and $\Omega_1 = d^{-\upsilon}$, $\Omega_2 = (1-d)^{-\upsilon}$.

Without loss of generality, we define that h_1 is subject to Rician fading with parameters K_1 and Ω_1 where K_1 is the Rician factor, while h_2 is subject to Rayleigh fading with parameter Ω_2. The PDF and CDF of α_1 are given in (1) and (2), respectively.

$$f_{\alpha 1}(x) = \frac{1+K_1}{\Omega_1} exp\left(-\frac{1+K_1}{\Omega_1}x - K_1\right) I_0\left(2\sqrt{\frac{K_1(1+K_1)}{\Omega_1}x}\right) \quad (1)$$

$$F_{\alpha 1}(x) = 1 - Q_1\left(\sqrt{2K_1}, \sqrt{\frac{2(1+K_1)}{\Omega_1}x}\right) \quad (2)$$

For Rayleigh fading, α_2 is an exponentially distributed RV, the PDF and CDF of α_2 are written as $f_{\alpha 2}(x) = \omega_2\, exp(-\omega_2 x)$, $F_{\alpha 2}(x) = 1 - exp(-\omega_2 x)$, where $\omega_2 = 1/\Omega_2$.

3. End-to-end Outage Probability Analysis

We consider four different APs at the relay. First, VG policy where R has full knowledge of h_1 and h_2. Second, FG policy where R only knows Ω_1 and Ω_2. Third, a mixed amplification (MA1) policy where h_1 and Ω_2 is available at R. Fourth, another mixed amplification (MA2) policy where h_2 and Ω_1 is available at R.

The end-to-end received SNR at N_i, γ_{Ni}, can be expressed as

$$\gamma_{Ni} = \rho q_k \alpha_i \alpha_k b_\Xi^2 / (1 + b_\Xi^2 \alpha_i) \tag{3}$$

where $i \in \{1,2\}$, $k = 3 - i$ and b_Ξ, $\Xi \in \{1,2,3,4\}$ is the amplification coefficient. The choice of b_Ξ under different APs is listed in **Table 1**.

Table 1. Amplification coefficients of different APs

AP	amplification coefficient b_Ξ
FG	$b_1 = \sqrt{\rho q_3 / (\rho q_1 \Omega_1 + \rho q_2 \Omega_2 + 1)}$
VG	$b_2 = \sqrt{\rho q_3 / (\rho q_1 \alpha_1 + \rho q_2 \alpha_2 + 1)}$
MA1	$b_3 = \sqrt{\rho q_3 / (\rho q_1 \alpha_1 + \rho q_2 \Omega_2 + 1)}$
MA2	$b_4 = \sqrt{\rho q_3 / (\rho q_1 \Omega_1 + \rho q_2 \alpha_2 + 1)}$

Hereinafter, for ease of notations, we define the following instantaneous and average received SNRs during the transmission, $\gamma_1 = \rho q_1 \alpha_1, \gamma_2 = \rho q_2 \alpha_2, \gamma_3 = \rho q_3 \alpha_1, \gamma_4 = \rho q_3 \alpha_2$, $\overline{\gamma_l} = E\{\gamma_l\}$, $l \in \{1,2,3,4\}$ is the expectation. In addition, $\vartheta_i = 1 + (q_i/q_3)$ is determined by power allocation policies. It is observed that, by choosing proper parameters, the exact expressions of end-to-end received SNR under different APs can be formulated uniformly as

$$\gamma_{eq} = \frac{\gamma_a \gamma_b}{\mu_a \gamma_a + \mu_b \gamma_b + c_\Xi} \tag{4}$$

where γ_{eq} denotes the equivalent end-to-end SNR, μ_a, μ_b are constants and γ_a, γ_b are instantaneous received SNRs during the transmission. Without loss of generality, let γ_a denote the Rician SNR as in (1) and (2) with parameters K_a and $\overline{\gamma_a}$, γ_b represents an Rayleigh SNR with $\overline{\gamma_b}$. The exact expression and uniform parameterization of end-to-end received SNR under different APs are presented in **Table 2**.

Table 2. Exact expression and uniform parameterization of end-to-end SNR

AP	FG		VG		MA1		MA2	
γ_{N1}	$\frac{\gamma_3\gamma_2}{\gamma_3 + c_1}$		$\frac{\gamma_3\gamma_2}{\vartheta_1\gamma_3 + \gamma_2 + c_2}$		$\frac{\gamma_3\gamma_2}{\vartheta_1\gamma_3 + c_3}$		$\frac{\gamma_3\gamma_2}{\gamma_3 + \gamma_2 + c_4}$	
γ_{N2}	$\frac{\gamma_1\gamma_4}{\gamma_4 + c_1}$		$\frac{\gamma_1\gamma_4}{\gamma_1 + \vartheta_2\gamma_4 + c_2}$		$\frac{\gamma_1\gamma_4}{\gamma_1 + \gamma_4 + c_3}$		$\frac{\gamma_1\gamma_4}{\vartheta_2\gamma_4 + c_4}$	
c_Ξ	$c_1 = 1 + \overline{\gamma_1} + \overline{\gamma_2}$		$c_2 = 1$		$c_3 = 1 + \overline{\gamma_2}$		$c_4 = 1 + \overline{\gamma_1}$	
	μ_a, μ_b	γ_a, γ_b	μ_a, μ_b	γ_a, γ_b	μ_a, μ_b	γ_a, γ_b	μ_a, μ_b	γ_a, γ_b
γ_{N1}	1, 0	γ_3, γ_2	ϑ_1, 1	γ_3, γ_2	ϑ_1, 0	γ_3, γ_2	1, 1	γ_3, γ_2
γ_{N2}	0, 1	γ_1, γ_4	1, ϑ_2	γ_1, γ_4	1, 1	γ_1, γ_4	0, ϑ_2	γ_1, γ_4

Furthermore, a uniform expression for the CDF of end-to-end SNRs under different APs is presented in the following proposition.

***Proposition 1*:** In TWAF relay networks operating over mixed Rician and Rayleigh fading channels, the exact CDF of γ_{eq}, $F_{eq}(\gamma_{th})$, is written as

$$F_{eq}(\gamma_{th}) = 1 - e^{-K_a - \Lambda\gamma_{th}} \sum_{m=0}^{\infty} \frac{2{K_a}^m}{(m!)^2} \sum_{p=0}^{m} C_m^p \, {\mu_b}^{m-p} (\lambda_a \gamma_{th})^{\frac{2m-p+1}{2}} \times [\lambda_b(\mu_a\mu_b\gamma_{th} + c_\Xi)]^{\frac{p+1}{2}} K_{p+1}\left(2\sqrt{\lambda_a\lambda_b(\mu_a\mu_b{\gamma_{th}}^2 + c_\Xi\gamma_{th})}\right) \quad (5)$$

where $\lambda_a = (1+K_a)/\overline{\gamma_a}$, $\lambda_b = 1/\overline{\gamma_b}$, $\Lambda = \lambda_a\mu_b + \lambda_b\mu_a$, C_m^p is the binomial coefficient.

***Proof*:** According to probability, $F_{eq}(\gamma)$ can be expressed as

$$F_{eq}(\gamma_{th}) = 1 - \int_{x=\mu_b\gamma_{th}}^{\infty} \tilde{F}_{\gamma b}\left(\frac{(\mu_a x + c_\Xi)\gamma_{th}}{x - \mu_b\gamma_{th}}\right) f_{\gamma a}(x)dx \quad (6)$$

Substitute (1) into this equation, expand $I_0(z)$ into series ([20], eq. (8.445)), use a change of variables $y = (x - \mu_b\gamma_{th})/\gamma_{th}$ and expand the power term into binomial form, we get

$$F_{eq}(\gamma_{th}) = 1 - \lambda_a e^{-K_a} \sum_{m=0}^{\infty} \frac{(K_a\lambda_a)^m}{(m!)^2} {\gamma_{th}}^{m+1} e^{-(\lambda_a\mu_b + \lambda_b\mu_a)\gamma_{th}} \sum_{p=0}^{m} C_m^p \, {\mu_b}^{m-p} \times \int_{y=0}^{\infty} exp\left(-\frac{\lambda_b(\mu_a\mu_b\gamma_{th} + c_\Xi)}{y} - \lambda_a\gamma_{th}y\right) y^p dy \quad (7)$$

The integral can be resolved in closed form ([18], eq. (3.471.9)). After rearrangement we get the desired result. ■

Concerning the convergence of the infinite series in (5), substitute an asymptotic expression for $K_v(z)$ ([15], eq. (15)), the residual of *M* terms truncation, R_M, is written as

$$R_M \approx e^{-K_a - \lambda_b\mu_a\gamma_{th}} \sum_{m=M}^{\infty} \frac{{K_a}^m}{(m!)^2} \sum_{p=0}^{m} \frac{m!\, e^{-\mu_b\lambda_a\gamma_{th}}}{(m-p)!} (\mu_b\lambda_a\gamma_{th})^{m-p} = e^{-K_a - \lambda_b\mu_a\gamma_{th}} \sum_{m=M}^{\infty} \frac{{K_a}^m}{(m!)^2} \Gamma(m+1, \mu_b\lambda_a\gamma_{th}) \quad (8)$$

It can be observed that $\Gamma(m+1, \mu_b\lambda_a\gamma_{th}) < \Gamma(m+1) = m!$ and $\lim_{x\to\infty} {K_a}^x/x! = 0$. As will be seen later, (5) converges quickly for a finite number of *M* terms thus truncation does not sacrifice numerical accuracy.

For certain special cases (5) could be simplified. For instance, when $\mu_b = 0$, $F_{eq}(\gamma_{th})$ is rewritten as

$$F_{eq}(\gamma_{th}) = 1 - e^{-K_a - \lambda_b\mu_a\gamma_{th}} \sum_{m=0}^{\infty} \frac{2{K_a}^m}{(m!)^2} (\lambda_a\lambda_b c_\Xi\gamma_{th})^{\frac{m+1}{2}} K_{m+1}\left(2\sqrt{\lambda_a\lambda_b c_\Xi\gamma_{th}}\right) \quad (9)$$

In communications system, the outage event is identified as the received SNR falls below a predetermined threshold, γ_{th}, i.e., $P_{out} = P\{\gamma_{eq} \le \gamma_{th}\} = F_{eq}\{\gamma_{th}\}$ which is the value of the CDF function at γ_{th}. In order to gain more insight we further investigate into the asymptotic behavior of the end-to-end OP in high SNR regime and present the following proposition.

***Proposition 2*:** With VG and FG polices, the asymptotic OP of the end-to-end transmission in

high SNR regime of the considered scenario is given is **Table 3.**

Table 3. upper bound of SNR and asymptotic end-to-end OP in high SNR regime

Link	Policy	SNR upper bound	Asymptotic outage probability
Forward Link	γ_{N2} VG	$min(\gamma_2/\vartheta_1, \gamma_3)$	$(\lambda_2\vartheta_1 + \lambda_3 e^{-K_1})\gamma_{th}$
	γ_{N2} FG	$min(\gamma_3\gamma_2/c_1, \gamma_2)$	$(1 - e^{-K_1}c_1\lambda_3 ln\lambda_2)\lambda_2\gamma_{th}$
Reverse Link	γ_{N1} VG	$min(\gamma_1/\vartheta_2, \gamma_4)$	$(\lambda_4 + \lambda_1\vartheta_2 e^{-K_1})\gamma_{th}$
	γ_{N1} FG	$min(\gamma_1\gamma_4/c_1, \gamma_1,)$	$(1 - c_1\lambda_4 ln\lambda_1)\lambda_1 e^{-K_1}\gamma_{th}$

***Proof*:** We apply an upper bound for the exact individual end-to-end SNR based on an inequality that for $a, b > 0$, $ab/(a+b) \leq min(a, b)$ always holds true. This method is widely adopted in the literature and calculating CDF of the obtained upper bound the finals results directly arise. For detailed derivation please refer to [11][13][14] and the reference therein. ■

In **Fig. 2**, we plot the OP of the end-to-end transmissions in the considered scenario as functions of d and ρ, respectively. Particularly, equal power allocation (EPA) is adopted, i.e., $q_1 = q_2 = q_3 = 1/3$, besides, M=20 terms truncation in (5) is adopted. In **Fig. 3**, we plot the exact and asymptotic end-to-end OP as functions of system SNR ρ.

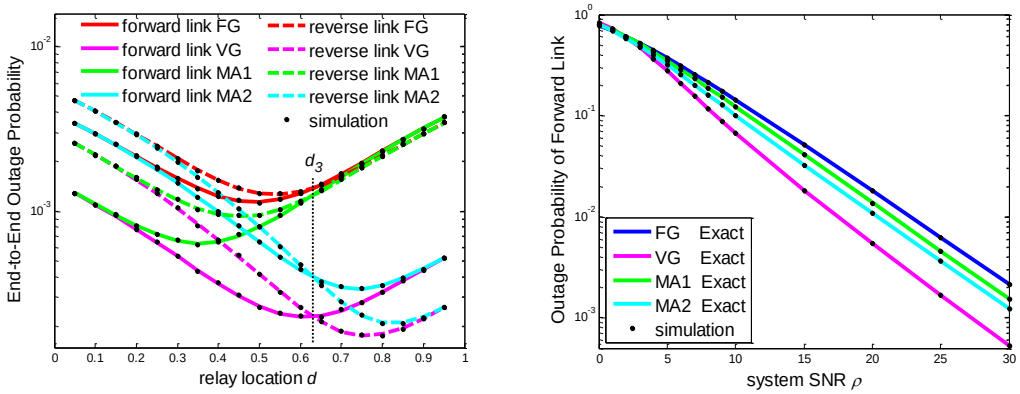

(a) end-to-end OP VS relay location d (b) end-to-end OP VS SNR ρ

Fig. 2. exact end-to-end outage probability with $\gamma_{th} = 1, \upsilon = 3, K_1 = 3$. (a):$\rho = 33$dB. (b):$d = 0.5$.

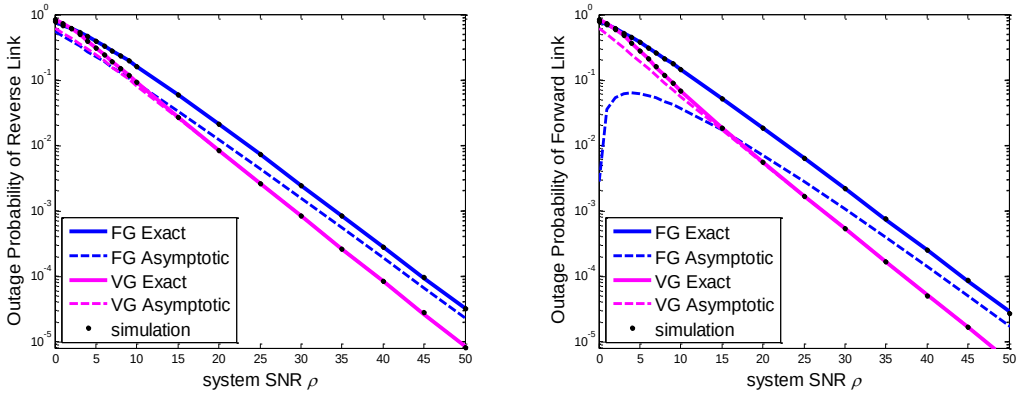

(a) reverse link OP VS SNR ρ (b) forward link OP VS SNR ρ

Fig. 3. exact and asymptotic end-to-end outage probability with $\gamma_{th} = 1$, $\upsilon = 3$, $K_1 = 3$, $d = 0.5$ with different APs (a): the reverse link. (b): the forward link.

As seen in **Fig. 2** and **Fig. 3**, the Monte-Carlo simulation results well matched the analytical results which corroborate the correctness of the analysis. In general, we see that VG provides the most desirable OP performance, FG suffers from obvious performance loss compared with VG, and they together may be viewed as upper and lower bounds for the performance of mixed APs. It can be observed that when the relay is located very close to one source node, the performance gain by acquiring the CSI of the other link at the relay is negligible, in such conditions *the CSI of the stronger link itself is sufficient to obtain similar performance with VG*. With $K_1 = 3$, the vertical black dotted line at $d_3 \approx 0.63$ represents a boundary for relay location, where $d < d_3$ guarantees a better performance of the forward link compared with the reverse link. For TWAF with homogenous Rayleigh/Rayleigh fading channels ($K_1 = 0$), we have $d_0 = 0.5$. In this sense, *the Rician channel is able to 'push' the relay more far away while maintaining a better forward link performance*. In fact, the value of d_K is associated with K_1, generally, d_K becomes larger with the increment of K_1 and the reason of this phenomenon shall be discussed in Section 4.3. Besides, we see that the asymptotic behavior with VG policy approaches the exact performance more quickly than FG policy, and there are more obvious vibrations in low SNR regime for the forward link than the reverse link. This phenomenon is caused by the channel asymmetry and different convergence speed for the series-form PDFs of the distribution for Rican and Rayleigh SNRs.

Though not our primary concern, we very briefly look into the topic of optimizing the end-to-end OP performance. Take the forward link with VG policy for example, from **Table 3**, substitute $\vartheta_2 = 1 + q_2/q_3$ therein it can be shown that in high SNR regime, the OP of the forward link is asymptotically approximated as

$$P_{fwd}^{VG}(\gamma_{th}) \approx \left(\frac{1}{q_3\Omega_2} + \frac{e^{-K_1}(1+K_1)}{\Omega_1}\frac{(q_2+q_3)}{q_1 q_3}\right)\frac{\gamma_{th}}{\rho}$$

The optimization problem under total power constraint can be written as

$$\boldsymbol{q}_{\boldsymbol{fwd}}^{\boldsymbol{VG}} = \arg\min_{\boldsymbol{q}} \left(\frac{1}{q_3\Omega_2} + \frac{e^{-K_1}(1+K_1)}{\Omega_1}\frac{(q_2+q_3)}{q_1 q_3}\right)\frac{\gamma_{th}}{\rho}$$
$$s.t.\ -q_1 < 0,\ -q_2 < 0,\ -q_3 < 0,\ q_1 + q_2 + q_3 - 1 = 0. \quad (11)$$

Based on partial derivative of q_2, it can be seen that the global optimizer lies on the boundary of $-q_2 < 0$. So we relax the constraint to $-q_2 \le 0$, and the optimal solution can be written as

$$\boldsymbol{q}_{\boldsymbol{fwd}}^{\boldsymbol{VG}} = \left[\frac{\sqrt{\omega_1/\omega_2}}{1+\sqrt{\omega_1/\omega_2}}; 0; \frac{1}{1+\sqrt{\omega_1/\omega_2}};\right] \quad (12)$$

With $q_2 = 0$ the TWAF relay network reduces to a conventional one-way relay network and no information can be acquired at N_1, this conflicts with the bidirectional transmission nature of two-way relay networks. However, we see that *in high SNR regime the OP performance of individual end-to-end link in TWAF relay network is up-bounded by that in OW relay network*.

4. Overall Outage Probability and Power Allocation

As aforementioned the OP performance of VG and FG policies may be viewed as bounds for MA1 and MA2, in this section we focus on the overall OP analysis and PA schemes for VG and FG policies. Since TWAF relay network carries two data streams of opposite directions concurrently, the system is in outage if either N_1 or N_2 is in outage. Besides, N_1 and N_2

may have different traffic requirements. Thus, the overall OP is defined as

$$P_{out} = P\{\gamma_{N1} < \gamma_{th1} \; or \; \gamma_{N2} < \gamma_{th2}\} = 1 - P\{\gamma_{N1} > \gamma_{th1} \; and \; \gamma_{N2} > \gamma_{th2}\} \tag{13}$$

where γ_{th1} and γ_{th2} denote the prescribed SNR threshold at N_1 and N_2, respectively, and define $\eta = \gamma_{th1}/\gamma_{th2}$ as traffic pattern indicator representing the level of traffic requirement asymmetry.

4.1. Overall OP and PA Schemes with VG Policy

With VG policy, in order to simplify the analysis, we give an asymptotic lower bound for the overall OP in the following proposition.

***Proposition 3*:** When two source nodes have non-identical traffic requirements, the overall OP of a TWAF relay network with VG policy can be lower bounded by

$$P_{out}^{lb} = \begin{cases} 1 - Q_1\left(\sqrt{2K_1}, \sqrt{\dfrac{2\lambda_{\alpha 1}\gamma_{th1}}{\rho q_3}}\right) exp\left(-\dfrac{\omega_2\gamma_{th1}\vartheta_1}{\rho q_2}\right), & Case1. \\ 1 - Q_1\left(\sqrt{2K_1}, \sqrt{\dfrac{2\lambda_{\alpha 1}\gamma_{th2}\vartheta_2}{\rho q_1}}\right) exp\left(-\dfrac{\omega_2\gamma_{th2}}{\rho q_3}\right), & Case2. \\ 1 - Q_1\left(\sqrt{2K_1}, \sqrt{\dfrac{2\lambda_{\alpha 1}\gamma_{th2}\vartheta_2}{\rho q_1}}\right) exp\left(-\dfrac{\omega_2\gamma_{th1}\vartheta_1}{\rho q_2}\right), & Case3. \end{cases} \tag{14}$$

where $\lambda_{\alpha 1} = (1 + K_1)/\Omega_1$, $\omega_2 = 1/\Omega_2$, $\zeta_1 = 1/(1 + \eta)$, $\zeta_2 = \eta/(1 + \eta)$, and Case1, Case2, and Case3 are characterized by $q_1 \geq \zeta_1$, $q_2 \geq \zeta_2$, and $(q_1 < \zeta_1, q_2 < \zeta_2)$, respectively.

And in high SNR regime an asymptotic expression of (14) is given by

$$P_{out}^{asymp} \approx \begin{cases} \dfrac{\eta\gamma_{th2}}{\rho}\left(\dfrac{\omega_1}{q_3} + \dfrac{\omega_2(q_1 + q_3)}{q_2 q_3}\right), & Case1. \\ \dfrac{\gamma_{th2}}{\rho}\left(\dfrac{\omega_1(q_2 + q_3)}{q_1 q_3} + \dfrac{\omega_2}{q_3}\right), & Case2. \\ \dfrac{\gamma_{th2}}{\rho}\left(\dfrac{\omega_1(q_2 + q_3)}{q_1 q_3} + \dfrac{\omega_2\eta(q_1 + q_3)}{q_2 q_3}\right), & Case3. \end{cases} \tag{15}$$

where $\omega_1 = e^{-K_1}(1 + K_1)/\Omega_1$.

***Proof*:** Apply the upper bound for end-to-end SNR from **Table 3**, wet get a lower bound of the OP for the reverse link as

$$P\{\gamma_{N1}^{ub} > \gamma_{th1}\} = P\left\{\alpha_1 > \frac{\eta\gamma_{th2}}{\rho q_3}\right\} P\left\{\alpha_2 > \frac{\vartheta_1\eta\gamma_{th2}}{\rho q_2}\right\} \tag{16}$$

Note that α_1 and α_2 are mutually independent. For the forward link we have

$$P\{\gamma_{N2}^{ub} > \gamma_{th2}\} = P\left\{\alpha_1 > \frac{\vartheta_2\gamma_{th2}}{\rho q_1}\right\} P\left\{\alpha_2 > \frac{\gamma_{th2}}{\rho q_3}\right\} \tag{17}$$

Note that if $q_1 < \zeta_1$, $\vartheta_2\gamma_{th2}/\rho q_1 > \eta\gamma_{th2}/\rho q_3$ holds and if $q_2 < \zeta_2$, $\vartheta_1\eta\gamma_{th2}/\rho q_2 > \gamma_{th2}/\rho q_3$ holds. Along with the total power constraint of $q_1 + q_2 + q_3 = 1$, (13) could be rewritten as

$$P_{out}^{lb}=\begin{cases}1-P\left\{\alpha_1>\dfrac{\eta\gamma_{th2}}{\rho q_3}\right\}P\left\{\alpha_2>\dfrac{\vartheta_1\eta\gamma_{th2}}{\rho q_2}\right\}, & q_1\geq\zeta_1.\\ 1-P\left\{\alpha_1>\dfrac{\vartheta_2\gamma_{th2}}{\rho q_1}\right\}P\left\{\alpha_2>\dfrac{\gamma_{th2}}{\rho q_3}\right\}, & q_2\geq\zeta_2.\\ 1-P\left\{\alpha_1>\dfrac{\vartheta_2\gamma_{th2}}{\rho q_1}\right\}P\left\{\alpha_2>\dfrac{\vartheta_1\eta\gamma_{th2}}{\rho q_2}\right\}, & q_1<\zeta_1,q_2<\zeta_2.\end{cases} \quad (18)$$

Substitute into (18) the CDF expressions for α_1 and α_2, we directly arrive at (14). It is interesting to see that if $q_1\geq\zeta_1$, the overall OP is determined by the reverse link itself. If $q_2\geq\zeta_2$, the forward link dominates. Only when $q_1<\zeta_1$, $q_2<\zeta_2$ holds simultaneously, the overall OP is codetermined by both links.

Substitute the well-known small value approximate for $I_0(z)$ ([21], eq. (9.6.7)) into ([22], eq. (4.41)), after some algebraic manipulations it can be shown that with α fixed and β approaches 0, we have

$$\lim_{\beta\to0}Q_1(\alpha,\beta)\approx1-\frac{\beta^2}{2}exp\left(-\frac{\alpha^2}{2}\right) \quad (19)$$

In high SNR regime, i.e., when $1/\rho\to0$, substituting (19) and $e^{-x}\approx1-x$ into (14) and omit the higher order infinitesimals directly yields (15). ■

Next, we present the optimal power allocation (OPA) scheme to minimize the asymptotic overall OP in (15). Obviously, under the total power constraint the following three cases should be considered.

Case1 ($q_1\geq\zeta_1$):

$$\boldsymbol{q}^*=\arg\min_{\boldsymbol{q}}\frac{\eta\gamma_{th2}}{\rho}\left(\frac{\omega_1}{q_3}+\frac{\omega_2(q_1+q_3)}{q_2q_3}\right)$$
$$s.t.\ -q_1\leq-\zeta_1,\ -q_2<0,\ -q_3<0,\ q_1+q_2+q_3-1=0. \quad (20)$$

Case2 ($q_2\geq\zeta_2$):

$$\boldsymbol{q}^*=\arg\min_{\boldsymbol{q}}\frac{\gamma_{th2}}{\rho}\left(\frac{\omega_1(q_2+q_3)}{q_1q_3}+\frac{\omega_2}{q_3}\right)$$
$$s.t.\ -q_2\leq-\zeta_2,\ -q_1<0,\ -q_3<0,\ q_1+q_2+q_3-1=0. \quad (21)$$

Case3 ($q_1<\zeta_1,q_2<\zeta_2$)

$$\boldsymbol{q}^*=\arg\min_{\boldsymbol{q}}\frac{\gamma_{th2}}{\rho}\left(\frac{\omega_1(q_2+q_3)}{q_1q_3}+\frac{\omega_2\eta(q_1+q_3)}{q_2q_3}\right)$$
$$s.t.\ q_1<\zeta_1,\ q_2<\zeta_2,\ -q_1<0,\ -q_2<0,\ -q_3<0,\ q_1+q_2+q_3-1=0. \quad (22)$$

It is interesting to see that, though via different methods, (18)-(20) bears basically similar mathematical forms with ([5], eq. (18, 22, 33)) which deals with TWAF relay network with VG policy under homogenous Rayleigh/Rayleigh fading channels, of course in our analysis the Rician channel introduces a new definition for ω_1. Following standard analysis and applying Lagrange dual method with Karush-Khun-Tucker (KKT) conditions to solve (20)-(22), we arrive at the following lemma.

Lemma 1: the OPA that minimize the asymptotic overall OP (15) of TWAF relay network with VG policy operating over mixed Rician and Rayleigh fading channels, under the total power constraint of $q_1+q_2+q_3=1$, $q_i>0$, $i=1,2,3$, is given by

$$\boldsymbol{q}^{opa}=\begin{cases}\boldsymbol{q}_{\boldsymbol{A}}^{*}=\left[\zeta_1;\dfrac{\omega_2}{\omega_2-\omega_1}\left(1-\sqrt{\dfrac{\omega_1\eta+\omega_2}{\omega_2(1+\eta)}}\right);\zeta_2-q_{a2};\right], & P_1\le 0,P_2>0\\ \boldsymbol{q}_{\boldsymbol{B}}^{*}=\left[\dfrac{\omega_1}{\omega_1-\omega_2}\left(1-\sqrt{\dfrac{\omega_1\eta+\omega_2}{\omega_1(1+\eta)}}\right);\zeta_2;\zeta_1-q_{b1};\right], & P_1>0,P_2\le 0\\ \boldsymbol{q}_{\boldsymbol{C}}^{*}=\left[\dfrac{1}{1+\phi_d+\sqrt{2\phi_d}};\dfrac{\phi_d}{1+\phi_d+\sqrt{2\phi_d}};\dfrac{\sqrt{2\phi_d}}{1+\phi_d+\sqrt{2\phi_d}};\right], & P_1>0,P_2>0\end{cases}\tag{23}$$

where $P_1=\phi_d+\sqrt{2\phi_d}-\eta$, $P_2=\eta\left(\sqrt{2\phi_d}+1\right)-\phi_d$, $\phi_d=\sqrt{\eta\omega_2/\omega_1}$. Note that if $\omega_1=\omega_2$, $\boldsymbol{q}_{\boldsymbol{A}}^{*}$ and $\boldsymbol{q}_{\boldsymbol{B}}^{*}$ reduces to $\boldsymbol{q}_{\boldsymbol{A}}^{*}=[\zeta_1;\zeta_2/2;\zeta_2/2;]$, $\boldsymbol{q}_{\boldsymbol{B}}^{*}=[\zeta_1/2;\zeta_2;\zeta_1/2;]$■

As a special case, in practical applications where equal source power (ESP) is mandated upon two source nodes, i.e., with an extra $q_1=q_2$ constraint, the optimal power allocation scheme with such constraint, OESP, is given by the following lemma.

***Lemma 2*:** The OESP that minimize the asymptotic system overall OP (15) of TWAF relay network with VG policy operating over mixed Rician and Rayleigh fading channels, where two source nodes are loaded with equal transmission power, is given by

$$\boldsymbol{q}^{oesp}=\begin{cases}\boldsymbol{q}_{\boldsymbol{D}}^{*}=\left[\dfrac{\Delta_d}{1+2\Delta_d};\dfrac{\Delta_d}{1+2\Delta_d};\dfrac{1}{1+2\Delta_d};\right], & 0<\eta\le\eta_a\\ \boldsymbol{q}_{\boldsymbol{E}}^{*}=\left[\dfrac{\Delta_e}{1+2\Delta_e};\dfrac{\Delta_e}{1+2\Delta_e};\dfrac{1}{1+2\Delta_e};\right], & \eta_a<\eta<\eta_b\\ \boldsymbol{q}_{\boldsymbol{F}}^{*}=\left[\dfrac{\Delta_f}{1+2\Delta_f};\dfrac{\Delta_f}{1+2\Delta_f};\dfrac{1}{1+2\Delta_f};\right], & \eta\ge\eta_b\end{cases}\tag{24}$$

where $\eta_a=\sqrt{0.5}/\left(1+\sqrt{0.5}\right)$, $\eta_b=1/\eta_a$, $\Delta_d=\sqrt{\omega_1/2(\omega_1+\omega_2)}$, $\Delta_e=\sqrt{0.5}$, $\Delta_f=\sqrt{\omega_2/2(\omega_1+\omega_2)}$. Note that when the relay is located too close to the source and thus rendering $\Delta_d/(1+2\Delta_d)<\zeta_2$, $\boldsymbol{q}_{\boldsymbol{D}}^{*}$ reduces to $\boldsymbol{q}_{\boldsymbol{D}}^{*}=[\zeta_2;\zeta_2;1-2\zeta_2;]$. Similarly, when $\Delta_f/\left(1+2\Delta_f\right)<\zeta_1$, $\boldsymbol{q}_{\boldsymbol{F}}^{*}$ reduces to $\boldsymbol{q}_{\boldsymbol{F}}^{*}=[\zeta_1;\zeta_1;1-2\zeta_1;]$.■

4.2 Overall OP and PA Scheme with FG Policy

In this subsection we redirect our attention to FG policy. According to probability, the overall outage could be written as [9]

$$\begin{aligned}P_{out}^{FG}&=Pr\{\gamma_{N1}<\gamma_{th1}\ or\ \gamma_{N2}<\gamma_{th2}\}\\&=\underbrace{Pr\{\gamma_{N1}<\gamma_{th1},\gamma_{N1}<\eta\gamma_{N2}\}}_{I_a}+\underbrace{Pr\{\gamma_{N2}<\gamma_{th2},\eta\gamma_{N2}<\gamma_{N1}\}}_{I_b}\end{aligned}\tag{25}$$

First we look into I_a. From **Table 2**, I_a could be expressed as

$$\begin{aligned}I_a&=Pr\left\{\frac{\rho^2q_2q_3\alpha_1\alpha_2}{\rho q_3\alpha_1+c_1}<\gamma_{th1},\frac{\rho^2q_2q_3\alpha_1\alpha_2}{\rho q_3\alpha_1+c_1}<\frac{\rho^2\eta q_1q_3\alpha_1\alpha_2}{\rho q_3\alpha_2+c_1}\right\}\\&=\int_{\delta_1}^{\delta_2}f_{\alpha_1}(x)\int_0^{T_1(x)}f_{\alpha_2}(y)\,dydx+\int_{\delta_2}^{\infty}f_{\alpha_1}(x)\int_0^{T_2(x)}f_{\alpha_2}(y)\,dydx\end{aligned}\tag{26}$$

Similarly, I_b could be expressed as

$$I_b=\int_{\delta_3}^{\delta_4}f_{\alpha2}(x)\int_0^{T_3(x)}f_{\alpha1}(y)\,dydx+\int_{\delta_4}^{\infty}f_{\alpha2}(x)\int_0^{T_4(x)}f_{\alpha1}(y)\,dydx\tag{27}$$

The integral boundaries in (27), (28) are defined as follows

$$\begin{cases} T_1(x) = \dfrac{\eta q_1}{q_2}x + \dfrac{c_1(\eta q_1 - q_2)}{\rho q_2 q_3}; T_2(x) = \dfrac{\gamma_{th1}}{\rho q_2}\left(1 + \dfrac{c_1}{\rho q_3 x}\right);\ T_3(x) = \dfrac{q_2}{\eta q_1}x + \dfrac{c_1(q_2 - \eta q_1)}{\rho \eta q_1 q_3}. \\ T_4(x) = \dfrac{\gamma_{th2}}{\rho q_1}\left(1 + \dfrac{c_1}{\rho q_3 x}\right); \delta_1 = \left[\dfrac{c_1(q_2 - \eta q_1)}{\rho \eta q_1 q_3}\right]^+ ;\ \delta_3 = \left[\dfrac{c_1(\eta q_1 - q_2)}{\rho q_2 q_3}\right]^+ \\ \delta_2 = \dfrac{q_3\gamma_{th1} + c_1(q_2 - \eta q_1) + \sqrt{[q_3\gamma_{th1} + c_1(q_2 - \eta q_1)]^2 + 4\eta q_1 q_3 c_1 \gamma_{th1}}}{2\rho\eta q_1 q_3} \\ \delta_4 = \dfrac{q_3\gamma_{th1} + c_1(\eta q_1 - q_2) + \sqrt{[q_3\gamma_{th1} + c_1(\eta q_1 - q_2)]^2 + 4 q_2 q_3 c_1 \gamma_{th1}}}{2\rho q_2 q_3} \end{cases}$$

It is difficult, if not impossible, for I_a and I_b to be resolved in closed form. In fact, after expanding the Marcum-Q function ([22], eq. (4.35)) and Bessel function ([20], eq. (8.447.1)) into infinite series, and with the aid of Taylor series, I_a and I_b can be expressed in multi-fold infinite series, which is not quite efficient for mathematical computation. Alternatively, we resort to numerical methods ([21], eq. (25.4.38)) to calculate I_a and I_b.

Take the second term of I_a for example, after simple manipulations we get

$$I_{a2} = \int_{\delta_2}^{\infty} f_{\alpha_1}(x) \int_0^{T_2(x)} f_{\alpha_2}(y)\, dydx = \int_0^{\frac{\pi}{2}} f_{\alpha_1}(tan\theta + \delta_2)\, F_{\alpha_2}\big(T_2(tan\theta + \delta_2)\big) sec^2\theta d\theta \quad (28)$$

Let $w_n = \pi/N_t$, $z_n = cos\,(2n-1)\pi/2N_t$, $c_n = sin\,(2n-1)\pi/2N_t$ $\theta_n = (z_n + 1)\,\pi/4$, $x_n = tan\theta_n + \delta_2$, (28) could be evaluated as

$$I_{a2} = \sum_{n=1}^{N_t} \frac{w_n f_{\alpha_1}(x_n) F_{\alpha_2}\big(T_2(x_n)\big) sec^2(\theta_n) c_n \pi}{4} \quad (29)$$

For space limitations we omit the overall expression for (25). In simulation experiments, the choice of N_t always guarantees the stability of 7th decimal place and it is noted that N_t is affected by the average channel power and path-loss exponent. In general, when the relay is close to source nodes, larger value of N_t should be utilized. The OPA and OESP schemes that minimizes the OP performance with FG policy can be obtained by numerically solving (25), via exhaustive search type algorithms.

4.3 Simulation Results of Overall OP with VG and FG polices

In this subsection, we carry out Monte Carlo simulation experiments to examine the analytical results presents in the previous two subsections.

In **Fig. 4** we plot the overall OP performance of different PA schemes in TWAF relay network with FG and VG policies when source nodes have non-identical traffic requirements. We can see that with both VG and FG policies, OPA brings the most desirable OP performance compared with OESP and EPA in medium and high SNR, irrespective of relay locations. And it is a surprise that OESP works just slightly better than EPA with VG policy, but with FG policy OESP obviously outperforms EPA.

In **Fig. 5** we plot the overall OP performance of VG and FG policies when h_1 is characterized by different Rician factors. In addition, we compare the system performance under the considered mixed Rican and Rayleigh fading scenario, with that of a homogeneous Rayleigh fading scenario ($K_1 = 0$). It can be observed that when two source nodes have identical traffic requirement, the performance of the homogeneous Rayleigh scenario is strictly 'symmetric' w.r.t. $d_0 = 0.5$, with both VG and FG policies. Besides, we also see that

with the increment of the Rician factor, both FG and VG policies achieve better performance and with large K_1 value, the OP of VG can be times better than FG. The vertical black dotted line d_K indicates the relay location where OESP best approaches OPA, i.e., at d_K we have $\boldsymbol{q}^{oesp} = \boldsymbol{q}^{opa}$ and it is an interesting turning point in the OP curve. At last, we note that when the relay is located very close to N_1, the performance of VG policy with different K_1 is not as clearly distinguished from each other as in FG policy. For the VG policy with large K_1 and the proposed OPA in (23), we do not see a 'best' relay location that provides the best overall OP performance. The overall OP performance is more like a monotonic decreasing function of relay location d.

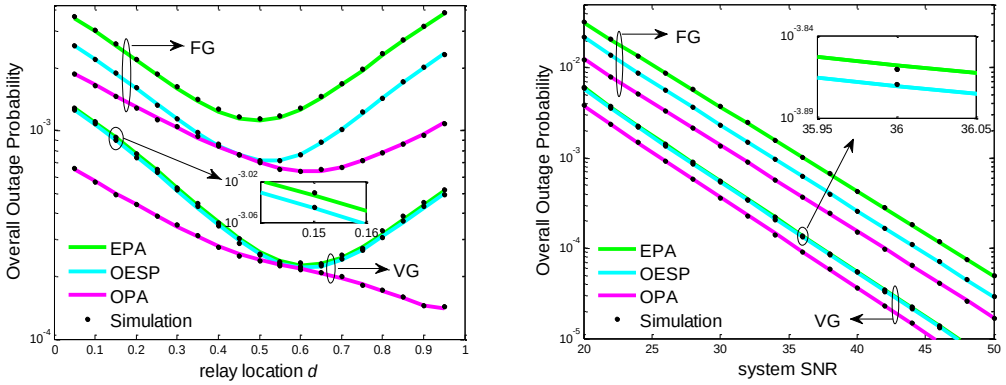

(a) Overall OP VS relay location d (b) Overall OP VS SNR ρ

Fig. 4. Overall OP of TWAF relay network with non-identical traffic requirements, $\gamma_{th1} = 0.5$, $\gamma_{th2} = 1$, $\eta = 0.5$, $\upsilon = 3$, $K_1 = 3$. (a): $\rho = 33$dB. (b): $d = 0.75$.

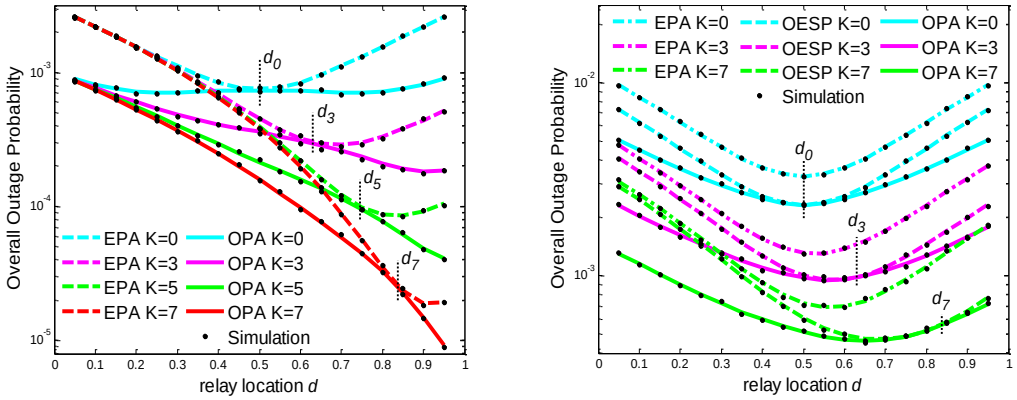

(a) Overall OP VS d with VG policy (b) Overall OP VS d with FG policy

Fig. 5. Overall OP of TWAF relay network with identical traffic requirements and different Rician factors, $\gamma_{th1} = \gamma_{th2} = 1$, $\eta = 1$, $\upsilon = 3$, $\rho = 33$dB. (a): With VG policy, $K_1 = 0,3,5,7$. (b): With FG policy, $K_1 = 0,3,7$.

In **Fig. 6** we plot the PA schemes presented in closed-form in (23) (24) for VG policy, and those acquired from exhaustive search type algorithms for FG policy, when two source nodes have equal traffic requirement. From (23) and (24), it can be proved that for a given η, d_K is the solution to $\phi_d = \sqrt{\eta\omega_2/\omega_1} = 1$ thus we have $d_K = 1/(1+\theta)$ where $\theta = \sqrt[\upsilon]{e^{-K_1}(1+K_1)/\eta}$. And from (12), we see that with EPA, a change of the worse

directional transmission link occurs if $(2-\eta)\omega_1 = (2\eta-1)\omega_2$ holds true, with $\eta = 1$, this point is also at d_K, that is why **Fig. 2(a)** and **Fig. 5** shares the same d_3. In this sense d_K represents a change of power allocation philosophy, to give more power to source node of the 'new' weaker link. Though theoretical expressions for PA schemes with FG is still missing, we see d_K applies to FG policy as well, at least roughly. Besides, we see that in high SNR regime FG policy always allocates more than half of the total power to the relay node, and both FG and VG policies share the same logic of allocating more power to the source node of weaker link.

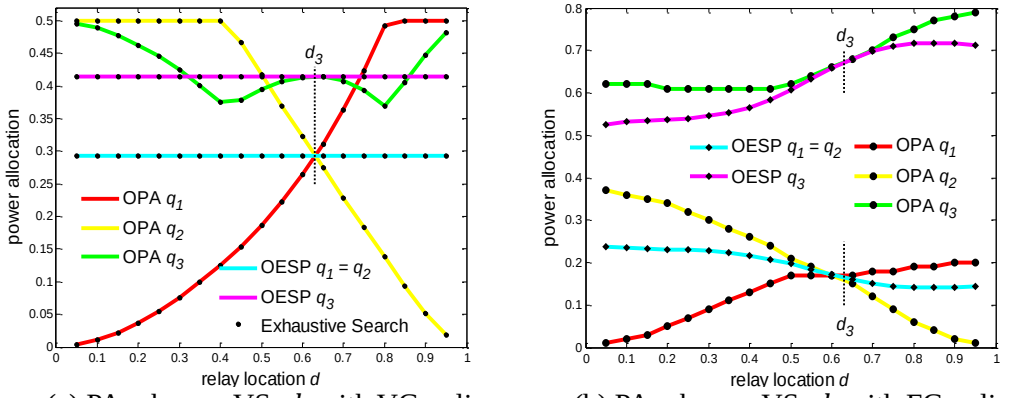

(a) PA schemes VS d with VG policy (b) PA schemes VS d with FG policy

Fig. 6. PA schemes of TWAF relay network, $\gamma_{th1} = \gamma_{th2} = 1$, $\eta = 1$, $\upsilon = 3$, $\rho = 33$dB, $K_1 = 3$. (a): closed-from solutions from (23) (24). (b): numerical solutions via exhaustive search.

5. Channel Capacity Analysis

In this section, we study the channel capacity of TWAF relay networks, with FG and VG policies, respectively. First, for each AP, we give tight lower bounds for the end-to-end links. Next, high SNR approximations were presented. At last, based on the high SNR approximations, we resort to numerical methods to obtain PA schemes that maximize the overall channel capacity under different constraints. We present the following lemma about the integral in the form $E\{ln(v_1\alpha_1 + v_2\alpha_2)\}$ $v_1 > 0, v_2 > 0$ which is needed in the following subsections.

***Lemma 3*:** If α_1 is a Rician Power RV with K_1 and Ω_1, α_2 is a Rayleigh Power RV with Ω_2, the integral $E\{ln(v_1\alpha_1 + v_2\alpha_2)\}$ $v_1 > 0, v_2 > 0$ can be resolved by

$$E\{ln(v_1\alpha_1 + v_2\alpha_2)\} = E_1(K_1) + ln(v_1 K_1/\lambda_{\alpha 1}) + \mathcal{J}(K_1, \theta) \tag{30}$$

where $\theta = v_1\omega_2/v_2\lambda_{\alpha 1}$, $\omega_2 = 1/\Omega_2$, $\lambda_{\alpha 1} = (1+K_1)/\Omega_1$ and $\mathcal{J}(a,x)$ is given by

$$\mathcal{J}(a,x) = \begin{cases} -e^{-a}\left(\dfrac{lnx}{1-x} + \displaystyle\sum_{n=1}^{\infty}\frac{a^n}{n!}\left[\frac{lnx}{(1-x)^{n+1}} + \sum_{m=1}^{n}\frac{1}{m}(1-x)^{m-n-1}\right]\right), & 0 < x < 1 \\ e^{-a}\displaystyle\sum_{n=1}^{\infty}\frac{a^{n-1}}{n!}x^{-n}\,{}_2F_1\left(n,n;n+1;1-\frac{1}{x}\right), & x > 1 \\ (1-e^{-a})/a\,, & x = 1 \end{cases} \tag{31}$$

***Proof*:** First, perform the integration w.r.t. α_2. With the aid of ([20], eq. (4.337.1)), we have

$$E\{ln(\nu_1\alpha_1+\nu_2\alpha_2)\}=\int_0^{\infty}\left(ln(\nu_1 x)+exp\left(\frac{\nu_1\omega_2 x}{\nu_2}\right)E_1\left(\frac{\nu_1\omega_2 x}{\nu_2}\right)\right)f_{\alpha 1}(x)dx \quad (32)$$

Substitute (1) herein and expand the Bessel function into series, (32) can be rewritten as

$$E\{ln(\nu_1\alpha_1+\nu_2\alpha_2)\}=E\{ln(\nu_1\alpha_1)\}+\lambda_{\alpha 1}e^{-K_1}\sum_{m=0}^{\infty}\frac{(K_1\lambda_{\alpha 1})^m}{(m!)^2}$$
$$\times\int_0^{\infty}E_1\left(\frac{\nu_1\omega_2}{\nu_2}x\right)exp\left(-\left(\lambda_{\alpha 1}-\frac{\nu_1\omega_2}{\nu_2}\right)x\right)x^m dx \quad (33)$$

The integral in (33) can be solved with the aid of ([23], eq. (4.1.8), (4.2.17), (4.2.20)) according to different values of $\theta=\nu_1\omega_2/\nu_2\lambda_{\alpha 1}$. Concerning the convergence of the infinite series, it will be shown later via simulations that a finite number of M terms truncation does not sacrifice numerical accuracy.■

5.1 Lower Bound and High SNR Approximation of Channel Capacity

In this subsection, we apply the method proposed by Zhong, etc. ([12], eq. (4)), which is a clever manipulation of Jensen's inequality, to present the lower bounds, and the method proposed by Rodríguez ([10], eq. (24)-(25)), to present the high SNR approximations. Though the lower bounds were originally proposed for FG policy, it can be extended to VG policy as well. We shall see that though via different methods, the results are closely related. In general, we have the following proposition.

Proposition 4: The lower bounds and high SNR approximations for the channel capacity of the end-to-end links in TWAF relay network operating over mixed Rician and Rayleigh fading channels, with both FG and VG polices, are given in **Table 4** with $\mathcal{F}_1(x)=ln(1+e^x)/2ln2$, $\mathcal{F}_2(x)=x/2ln2$, $c_1=1+\rho q_1\Omega_1+\rho q_2\Omega_2$, $\widetilde{c_1}=\rho q_1\Omega_1+\rho q_2\Omega_2$.

Table 4. Lower bounds and high SNR approximations of channel capacity

AP	**FG**		**VG**	
Link	reverse	forward	reverse	forward
Lower Bound	$\mathcal{F}_1(P_3(c_1))$	$\mathcal{F}_1(P_4(c_1))$	$\mathcal{F}_1(P_5)$	$\mathcal{F}_1(P_6)$
Approximate	$\mathcal{F}_2(P_3(\widetilde{c_1}))$	$\mathcal{F}_2(P_4(\widetilde{c_1}))$	$\mathcal{F}_2(P_5)$	$\mathcal{F}_2(P_6)$

$P_3(a)$, $P_4(a)$, P_5 and P_6 are defined as

$$\begin{cases}P_3(a)=-\mathcal{E}+E_1(K_1)+ln\dfrac{K_1}{a\lambda_1\lambda_2}-e^{a\lambda_3-K_1}\left[\sum_{m=0}^{M-1}\dfrac{{K_1}^m}{m!}\sum_{p=1}^{m+1}E_p(a\lambda_3)+\Delta(a,M,K_1)\right]\\ P_4(a)=-\mathcal{E}+E_1(K_1)+ln\dfrac{K_1}{a\lambda_1\lambda_4}-e^{a\lambda_4}E_1(a\lambda_4)\\ P_5=-\mathcal{E}-ln\vartheta_1\lambda_2+\mathcal{J}(K_1,\theta_1)\\ P_6=-\mathcal{E}-ln\lambda_4+\mathcal{J}(K_1,\theta_2)\end{cases}$$

where $\Delta(a,M,K_1)=E_1(a\lambda_3)e^{K_1}[\Upsilon(M-1,K_1)(M-1)K_1+\Upsilon(M,K_1)]/\Gamma(M)$, $\theta_1=\vartheta_1\lambda_2/\lambda_3$, $\theta_2=\lambda_4/\vartheta_2\lambda_1$ and $\mathcal{J}(a,x)$ is given in (31).

***Proof*:** For simplicity, take the reverse link for example. For lower bounds, applying Zhong's method ([12], eq. (4)), the lower bound of the reverse link with FG policy can be written as

$$C_{rvs}^{FG-lb} = \frac{1}{2} log_2\left(1 + exp(E\{ln\gamma_2\} + E\{ln\gamma_3\} - E\{ln(\gamma_3 + c_1)\})\right) \quad (34)$$

and for VG policy, let $c_2 = 0$ which is efficient in medium and high SNRs, the lower bound can be written as

$$C_{rvs}^{VG-lb} = \frac{1}{2} log_2\left(1 + exp(E\{ln\gamma_2\} + E\{ln\gamma_3\} - E\{ln(\vartheta_1\gamma_3 + \gamma_2)\})\right) \quad (35)$$

As for high SNR approximations, according to ([10], eq. (24)-(25)), the high SNRs approximations of channel capacity can be written as

$$\begin{cases} C_{rvs}^{VG} \approx \dfrac{1}{2ln2}\left(ln(\rho q_2 q_3) + E\{ln\alpha_1\} + E\{ln\alpha_2\} - E\{ln(q_2\alpha_2 + (q_1 + q_3)\alpha_1)\}\right) \\ C_{rvs}^{FG} \approx \dfrac{1}{2ln2}\left(ln\left(\rho q_2 q_3\right) + E\{ln\alpha_1\} + E\{ln\alpha_2\} - E\left\{ln\left(q_3\alpha_1 + q_1\Omega_1 + q_2\Omega_2\right)\right\}\right) \end{cases} \quad (36)$$

To evaluate (36)-(38), note that for Rayleigh fading, the integral $E\{ln\alpha_2\}$ and $E\{ln(a + \alpha_2)\}, a > 0$ were given in ([10], eq. (9)-(10)). And for Rician fading, $E\{ln\alpha_1\}$ and $E\{ln(a + \alpha_1)\}, a > 0$ were given in ([12], eq. (43), (47)). Therefore, the key task is to evaluate the integral in (30). Substitute (31) into (34)-(36) yields the desired result.■

5.2 Simulation Results of Channel Capacity

In this subsection, we resort to simulation experiments to validate the analytical results. The same as before, we use exhaustive search type algorithms to find the global optimizers that maximizes the sum capacity $C_{sum}^{AP} = C_{rvs}^{AP} + C_{fwd}^{AP}$ under the total power constraint (OPA) and equal source power constraint (OESP), respectively, and compare them to EPA. Note that $M \leq 20$ terms truncation is applied when calculating the functions defined in **Table 4**.

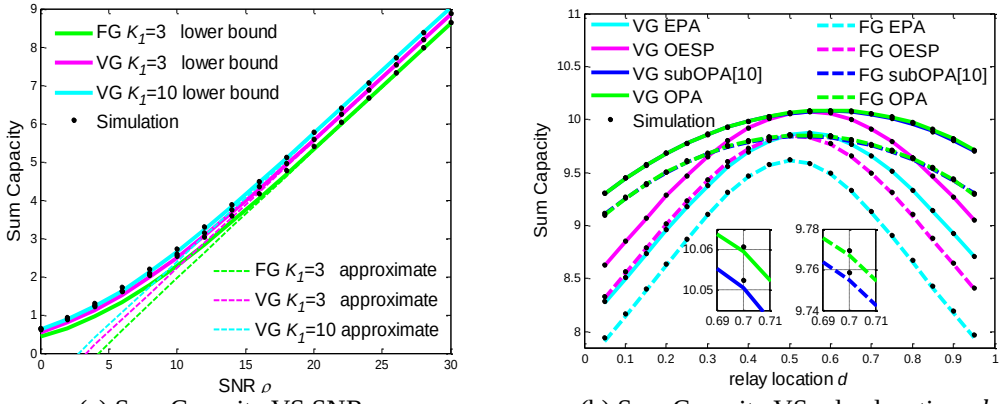

(a) Sum Capacity VS SNR ρ (b) Sum Capacity VS relay location d

Fig. 7. Sum capacity of TWAF relay network with VG and FG polices. $\upsilon = 3$. (a): $d = 0.5$. (b): $K_1 = 3$, $\rho = 33$dB.

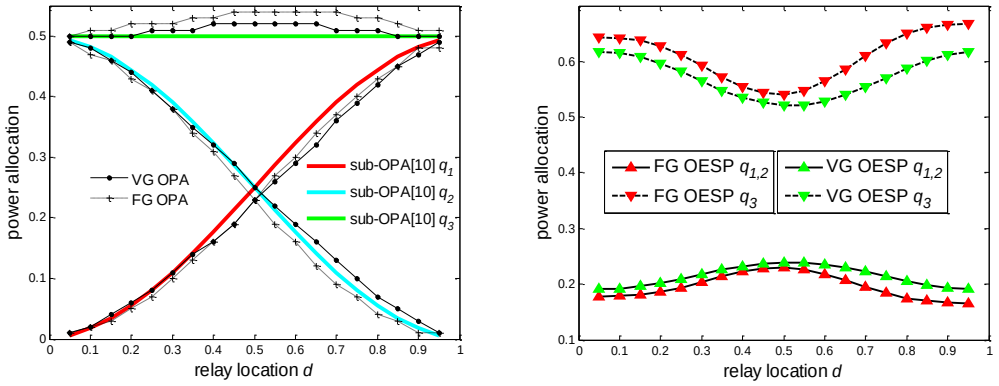

(a) OPA schemes VS relay location d (b) OESP schemes VS relay location d

Fig. 8. Power allocation schemes via exhaustive search to maximize sum capacity with VG and FG polices. $\upsilon = 3,\ K_1 = 3,\ \rho = 33$dB. (a): OPA schemes. (b): OESP schemes.

In **Fig. 7**, we plot the system sum capacity of TWAF relay network against SNR and relay location, respectively. In **Fig. 8**, we plot the OPA and OESP schemes obtained via exhaustive search type algorithms that maximize the sum capacity. As shown in **Fig. 7(a)**, the lower bounds and high SNR approximations of sum capacity are in fine agreement with the simulation results, especially in medium and high SNRs. In addition, we see that the sum capacity with VG policy is better than FG, and with the increment of K_1, the sum capacity slowly grows. However, in general the capacity performance is less sensitive to the increment of Rician factor compared with outage probability. In **Fig. 7(b)**, we compare the sum capacity of different PA schemes. It is noteworthy that the performance of OPA obtained via exhaustive search is, to a large extent, slightly better than and generally very similar to that of the sub-optimal scheme (sub-OPA) proposed in [10]. Though sub-OPA was originally proposed in a homogenous Rayleigh/Rayleigh fading scenario, it is solely determined by statistical channel powers and therefore to some extent it is "fading irrelevant". Furthermore, the OESP with both FG and VG policies obviously outperforms the EPA scheme, and still suffers from considerable performance loss compared with the OPA scheme. As seen in **Fig. 8**, the OPA and OESP schemes for FG and VG polices share the same trend as d varies from 0 to 1, and the sub-OPA scheme are very similar with the OPA scheme.

6. Conclusions

In this paper, we focus on analyzing and optimizing the OP and channel capacity of TWAF relay network operating over mixed Rician and Rayleigh fading channels, with different APs adopted at the relay, respectively. First, a uniform expression for the exact OP of end-to-end links which applies to different APs and simplified asymptotic expressions of for VG and FG policies were presented. Next, we investigated into the system overall OP with two source nodes having non-identical traffic requirements, under FG and VG polices, respectively. We were able to derive theoretical global optimizers for the overall OP with VG policy, while for FG policy we resort to numerical exhaustive search methods. Concerning channel capacity with both FG and VG polies, we presented explicit expressions for tight lower bounds and high SNR approximations of end-to-end links and then utilized them to search for the global optimizers that maximize the sum capacity. Extensive simulation experiments

were carried out to validate the analytical results and demonstrated that the proposed OPA and OESP schemes offer substantial performance improvements as compared to EPA scheme.

References

[1] B. Rankov and A. Wittneben, "Spectral efficient protocols for half-duplex fading relay channels," *IEEE J. Sel. Areas Commun.*, vol. 25, no. 2, pp. 379-389, February, 2007. Article (CrossRef Link).

[2] L. J. Rodríguez, N. Tran and T. Le-Ngoc, "Achievable rates and power allocation for two-way AF relaying over Rayleigh fading channels," in *Proc. of IEEE Int. Conf. Communications (ICC)*, pp. 5914-5918, June 9-13, 2013. Article (CrossRef Link).

[3] D. Li and K. Xiong, "SER analysis of physical layer network coding over Rayleigh fading channels with QPSK modulation," *Information-An International Interdisciplinary Journal*, vol. 15, no. 11(A), pp. 4573-4578, November, 2012.

[4] P. K. Upadhyay and S. Prakriya, "Performance of analog network coding with asymmetric traffic requirements," *IEEE Commun. Lett.*, vol. 15, no. 6, pp. 647-649, June, 2011. Article (CrossRef Link).

[5] X. Ji, B. Zheng, Y. Cai and L. Zou, "On the study of half-duplex asymmetric two-way relay transmission using an amplify-and-forward relay," *IEEE Trans. Veh. Technol.*, vol. 61, no. 4, pp. 1649-1664, May, 2012. Article (CrossRef Link).

[6] C. Zhang, J. Ge, J. Li and Y. Hu, "Performance evaluation for asymmetric two-way AF relaying in Rician fading," *IEEE Wireless Commun. Lett.*, vol. 2, no. 3, June, 2013. Article (CrossRef Link).

[7] J. Yang, P. Fan, Trung Q. Duong and X. Lei, "Exact performance of two-way AF relaying in Nakagami-m fading environment," *IEEE Trans. Wireless Commun.*, vol. 10, no. 3, pp. 980-987, March, 2011. Article (CrossRef Link).

[8] F. Xu, Francis C. M. Lau and D. Yue, "Diversity order for amplify-and-forward dual hop systems with fixed-gain relay under Nakagami fading channels," *IEEE Trans. Wireless Commun.*, vol. 9, no. 1, pp. 92-98, January, 2010. Article (CrossRef Link).

[9] Z. Ni, X. Zhang and D. Yang, "Outage performance of two-way fixed gain amplify-and-forward relaying systems with asymmetric traffic requirements," *IEEE Commun. Lett.*, vol. 18, no. 1, pp. 78-81, January, 2014. Article (CrossRef Link).

[10] L. J. Rodríguez, N. H. Tran and T. Le-Ngoc, "Achievable rate and power allocation for single-relay AF systems over Rayleigh fading channels at high and low SNRs," *IEEE Trans. Veh. Technol.*, vol. 63, no. 4, pp. 1726-1739, May, 2014. Article (CrossRef Link).

[11] K. Xiong, Q. Shi, P. Fan and K. B. Letaief, "Resource allocation for two-way relay networks with symmetric data rates: an information theoretic approach," in *Proc. of IEEE Int. Conf. Communications (ICC)*, pp. 6060-6064, June 9-13, 2013. Article (CrossRef Link).

[12] C. Zhong, M. Matthaiou, G. K. Karagiannidis and T. Ratnarajah, "Generic ergodic capacity bounds for fixed-gain AF dual-hop relaying systems," *IEEE Trans. Veh. Technol.*, vol. 60, no. 8, pp. 3814-3824, October, 2011. Article (CrossRef Link).

[13] O. Waqar, M. Ghogho and D. McLernon, "Tight bounds for ergodic capacity of dual-hop fixed-gain relay networks under Rayleigh fading," *IEEE Commun. Lett.*, vol. 15, no. 4, pp. 413-415, April, 2011. Article (CrossRef Link).

[14] S. S. Soliman and N. C. Beaulieu, "The bottleneck effect of Rician fading in dissimilar dual-hop AF relaying systems," *IEEE Trans. Veh. Technol.*, vol 63, no. 4, pp. 1957-1965, May, 2014. Article (CrossRef Link).

[15] M. R. Bhatnagar and M. K. Arti, "Performance analysis of AF based hybrid satellite-terrestrial cooperative network over generalized fading channels," *IEEE Commun. Lett.*, vol. 17, no. 10, pp. 1912-1915, October, 2013. Article (CrossRef Link).

[16] K. P. Peppas, G. C. Alexandropoulos and P. T. Mathiopoulos, "Performance analysis of dual-hop

AF relaying systems over mixed $\eta-\mu$ and $\kappa-\mu$ fading channels," *IEEE Trans. Veh. Technol.*, vol. 62, no. 7, pp. 3149-3163, September, 2013. Article (CrossRef Link).

[17] H. A. Suraweera, H. Y. Louie, Y. Li, G. K. Karagiannidis and B. Vucetic, "Two hop amplify-and-forward transmission in mixed Rayleigh and Rician fading channels," *IEEE Commun. Lett.*, vol. 13, no. 4, pp. 227-229, April, 2009. Article (CrossRef Link).

[18] H. A. Suraweera, G. K. Karagiannidis and P. J. Smith, "Performance analysis of the dual-hop asymmetric fading channel," *IEEE Trans. Wireless Commun.*, vol. 8, no. 6, pp. 2783-2788, June, 2009. Article (CrossRef Link).

[19] Z. Fan, D. Guo, B. Zhang and L. Zeng, "Performance analysis and optimization for AF two-way relaying with relay selection over mixed Rician and Rayleigh fading," *KSII Transactions on Internet and Information Systems*, vol. 6, no. 12, pp.3275-3295, December, 2012. Article (CrossRef Link).

[20] I. S. Gradshteyn and I. M. Ryzhik, *Table of Integrals, Series, and Products*, 7th Edition, Academic Press, San Diego, CA, 2007.

[21] M. Abramowitz and I. A. Stegun, *Handbook of Mathematical Functions with Formulas, Graphs, and Mathematical Tables*, 10th Edition, New York, Dover, 1972.

[22] M. K. Simon and M. S. Alouini, *Digital Communication over Fading Channels*, 2nd Edition, Wiley & Sons, New Jersey, 2005.

[23] I. S. Gradshteyn and I. M. Ryzhik, *Table of Integrals, Series, and Products*, 7th Edition, Academic Press, San Diego, CA, 2007.

[24] Murray Geller and Edward W. Ng, "A table of integrals of the exponential integral," Journal of Research of the National Bureau of Standards-B: Mathematics and Mathematical Science, vol. 73B, no. 3, pp. 191-210, July, 1969.

Qi Yanyan was born in 1985. He received the Master Degree in Enginnering in 2010 from North China Electric Power University. He is currently a Ph.D. candidate at Beijing University of Posts and Telecommunications, Beijing, China. His research interests include cooperative relay communications, multi-media communications and signal processing.

Wang Xiaoxiang was born in 1969. Prof. Wang is doctor supervisor in school of information and telecommunication Engineering. She received her PH.D. degree from BIT in 1998. She was a visit scholar in Austria University of Technology in Vienna from 2001 to 2002. Her research interests include cooperative communications, MIMO & OFDM technique, and MBMS systems.